EFFECTS OF RANDOM EDGE-DROPPING ON OVER-SQUASHING IN GRAPH NEURAL NETWORKS

Jasraj Singh*, **Keyue Jiang**, **Brooks Paige** & **Laura Toni**
University College London
{jasraj.singh.23,keyue.jiang.18,b.paige,l.toni}@ucl.ac.uk

ABSTRACT

Message Passing Neural Networks (MPNNs) are a class of Graph Neural Networks (GNNs) that leverage the graph topology to propagate messages across increasingly larger neighborhoods. The message-passing scheme leads to two distinct challenges: *over-smoothing* and *over-squashing*. While several algorithms, e.g. DropEdge and its variants – DropNode, DropAgg and DropGNN – have successfully addressed the over-smoothing problem, their impact on over-squashing remains largely unexplored. This represents a critical gap in the literature as failure to mitigate over-squashing would make these methods unsuitable for long-range tasks. In this work, we take the first step towards closing this gap by studying the aforementioned algorithms in the context of over-squashing. We present novel theoretical results that characterize the negative effects of DropEdge on sensitivity between distant nodes, suggesting its unsuitability for long-range tasks. Our findings are easily extended to its variants, allowing us to build a comprehensive understanding of how they affect over-squashing. We evaluate these methods using real-world datasets, demonstrating their detrimental effects. Specifically, we show that while DropEdge-variants improve test-time performance in short-range tasks, they deteriorate performance in long-range ones. Our theory explains these results as follows: random edge-dropping lowers the effective receptive field of GNNs, which although beneficial for short-range tasks, misaligns the models on long-range ones. This forces the models to overfit to short-range artefacts in the training set, resulting in poor generalization. Our conclusions highlight the need to re-evaluate various methods designed for training deep GNNs, with a renewed focus on modelling long-range interactions.

1 INTRODUCTION

Graph-structured data is ubiquitous – it is found in social media platforms, online retail platforms, molecular structures, transportation networks, and even computer systems. *Graph neural networks* (GNNs) (Li et al., 2016; Scarselli et al., 2009) are powerful neural models developed for modelling graph-structured data, and have found applications in several real-world scenarios (Gao et al., 2018; Monti et al., 2017; Wale & Karypis, 2006; Ying et al., 2018; You et al., 2020a;b;c; 2022; Zheng et al., 2022; Zitnik & Leskovec, 2017). A popular class of GNNs, called *message-passing neural networks* (MPNNs) (Gilmer et al., 2017), recursively process neighborhood information using message-passing layers. These layers are stacked to allow each node to aggregate information from increasingly larger neighborhoods, akin to how *convolutional neural networks* (CNNs) learn hierarchical features for images (LeCun et al., 1989). However, unlike in image-based deep learning, where *ultra-deep* CNN architectures have led to performance breakthroughs (He et al., 2016; Szegedy et al., 2015), shallow GNNs often outperform deeper models on many graph learning tasks (Zhou et al., 2021). This is because deep GNNs suffer from unique issues like *over-smoothing* (Oono & Suzuki, 2020) and *over-squashing* (Alon & Yahav, 2021), which makes training them notoriously difficult.

Over-smoothing refers to the problem of node representations becoming *too similar* as they are recursively processed. This is undesirable since it limits the GNN from effectively utilizing the

*Corresponding Author

information in the input features. The problem has garnered significant attention from the research community, resulting in a suite of algorithms designed to address it (Rusch et al., 2023). Amongst these methods are a collection of random edge-dropping algorithms, including DropEdge (Rong et al., 2020) and its variants – DropNode (Feng et al., 2020), DropAgg (Jiang et al., 2023) and DropGNN (Papp et al., 2021) – which act as *message-passing reducers*.

The other issue specific to GNNs is over-squashing. In certain graph structures, neighborhood size grows exponentially with distance from the source (Chen et al., 2018b), causing information to be lost as it passes through graph bottlenecks (Alon & Yahav, 2021). This limits MPNNs' ability to enable communication between distant nodes, which is crucial for good performance on long-range tasks. To alleviate over-squashing, several graph-rewiring techniques have been proposed, which aim to improve graph connectivity by adding edges in a strategic manner[1] (Alon & Yahav, 2021; Black et al., 2023; Deac et al., 2022; Karhadkar et al., 2023; Nguyen et al., 2023). In contrast, the DropEdge-variants only remove edges, which should, in principle, amplify over-squashing levels.

The empirical evidence in support of methods designed for training deep GNNs has been majorly collected on short-range tasks. That is, it simply suggests that *these methods prevent loss of local information, but it remains inconclusive if they facilitate capturing long-range interactions (LRIs)*. Of course, on long-range tasks, deeper GNNs are useless if they cannot capture LRIs. This is especially a concern for DropEdge-variants since evidence suggests that alleviating over-smoothing with graph rewiring could exacerbate over-squashing (Giraldo et al., 2023; Nguyen et al., 2023).

Theoretical Contributions. In this work, we uncover the effects of random edge-dropping algorithms on over-squashing in MPNNs. By explicitly computing the expected *sensitivity* of the node representations to the node features (Topping et al., 2022) (inversely related to over-squashing) in a linear GCN (Kipf & Welling, 2017), we show that these methods provably reduce the *effective receptive field* of the model. Precisely speaking, the rate at which sensitivity between distant nodes decays is *polynomial* w.r.t. the dropping probability. Finally, we extend the existing theoretical results on sensitivity in nonlinear MPNNs (Black et al., 2023; Di Giovanni et al., 2023; Xu et al., 2018) to the random edge-dropping setting, again showing that these algorithms exacerbate the over-squashing problem.

Experimental Results. We evaluate the DropEdge-variants on node classification tasks using GCN and GAT (Veličković et al., 2018) architectures. Specifically, we assess their performance on homophilic datasets – Cora (McCallum et al., 2000) and CiteSeer (Giles et al., 1998) – which represent short-range tasks, and heterophilic datasets – Chameleon, Squirrel, TwitchDE (Rozemberczki et al., 2021) – which correspond to long-range tasks. Our results indicate an increasing trend in test accuracy for homophilic datasets and a declining trend for heterophilic datasets as the dropping probability increases. Accordingly, we hypothesize that edge-dropping algorithms improve performance on short-range tasks, as has been reported earlier, by reducing the receptive field of the GNN and increasing model-dataset alignment, However, for long-range tasks, they decrease the model-dataset alignment, resulting in poor generalization.

2 Background

Consider a directed graph $\mathcal{G} = (\mathcal{V}, \mathcal{E})$, with $\mathcal{V} = [N] \coloneqq \{1, \dots, N\}$ denoting the node set and $\mathcal{E} \subset \mathcal{V} \times \mathcal{V}$ the edge set; $(j \to i) \in \mathcal{E}$ if there's an edge from node j to node i. Let $\boldsymbol{A} \in \{0,1\}^{N \times N}$ denote its adjacency matrix, such that $\boldsymbol{A}_{ij} = 1$ if and only if $(j \to i) \in \mathcal{E}$, and let $\boldsymbol{D} \coloneqq \operatorname{diag}(\boldsymbol{A}\mathbf{1}_N)$ denote the in-degree matrix. The geodesic distance, $d_{\mathcal{G}}(j, i)$, from node j to node i is the length of the shortest path starting at node j and ending at node i. Accordingly, the ℓ-hop neighborhood of a node i can be defined as the set of nodes that can reach it in exactly $\ell \in \mathbb{N}_0$ steps, $\mathbb{S}^{(\ell)}(i) = \{j \in \mathcal{V} : d_{\mathcal{G}}(j, i) = \ell\}$.

2.1 Graph Neural Networks

Graph neural networks (GNNs) operate on inputs of the form $(\mathcal{G}, \boldsymbol{X})$, where $\mathcal{G}$ encodes the graph topology and $\boldsymbol{X} \in \mathbb{R}^{N \times H^{(0)}}$ collects the node features[2]. Message-passing neural networks

[1] Sometimes, along with removal of some edges to preserve statistical properties of the original topology.

[2] To keep things simple, we will ignore edge features.

(MPNNs) (Gilmer et al., 2017) are a special class of GNNs which recursively aggregate information from the 1-hop neighborhood of each node using *message-passing layers*. An L-layer MPNN is given as

$$\begin{aligned} \boldsymbol{z}_i^{(\ell)} &= \mathsf{Upd}^{(\ell)}\left(\boldsymbol{z}_i^{(\ell-1)}, \mathsf{Agg}^{(\ell)}\left(\boldsymbol{z}_i^{(\ell-1)}, \left\{\boldsymbol{z}_j^{(\ell-1)} : j \in \mathbb{S}^{(1)}(i)\right\}\right)\right), \quad \forall \ell \in [L] \\ \mathsf{MPNN}_\theta(\mathcal{G}, \boldsymbol{X}) &= \left\{\mathsf{Out}\left(\boldsymbol{z}_i^{(L)}\right) : i \in \mathcal{V}\right\} \end{aligned} \tag{2.1}$$

where $\boldsymbol{Z}^{(0)} = \boldsymbol{X}$, $\mathsf{Agg}^{(\ell)}$ denotes the *aggregation functions*, $\mathsf{Upd}^{(\ell)}$ the *update functions*, and Out the *readout function*. Since the final representation of node i is a function of the input features of nodes at most L-hops away from it, its *receptive field* is given by $\mathbb{B}^{(L)}(i) := \{j \in \mathcal{V} : d_{\mathcal{G}}(j,i) \leq L\}$.

For example, a GCN (Kipf & Welling, 2017) updates node representations as the weighted sum of its neighbors' representations:

$$\boldsymbol{Z}^{(\ell)} = \sigma\left(\hat{\boldsymbol{A}}\boldsymbol{Z}^{(\ell-1)}\boldsymbol{W}^{(\ell)}\right) \tag{2.2}$$

where σ is a point-wise nonlinearity, e.g. ReLU, the propagation matrix, $\hat{\boldsymbol{A}}$, is a *graph shift operator*, i.e. $\hat{\boldsymbol{A}}_{ij} \neq 0$ if and only if $(j \to i) \in \mathcal{E}$ or $i = j$, and $\boldsymbol{W}^{(\ell)} \in \mathbb{R}^{H^{(\ell-1)} \times H^{(\ell)}}$ is a weight matrix. The original choice for $\hat{\boldsymbol{A}}$ was the symmetrically normalized adjacency matrix $\hat{\boldsymbol{A}}^{\text{sym}} := \widetilde{\boldsymbol{D}}^{-1/2}\widetilde{\boldsymbol{A}}\widetilde{\boldsymbol{D}}^{-1/2}$ (Kipf & Welling, 2017), where $\widetilde{\boldsymbol{A}} = \boldsymbol{A} + \boldsymbol{I}_N$ and $\widetilde{\boldsymbol{D}} = \text{diag}(\widetilde{\boldsymbol{A}}\boldsymbol{1}_N)$. However, several influential works have also used the asymmetrically normalized adjacency, $\hat{\boldsymbol{A}}^{\text{asym}} := \widetilde{\boldsymbol{D}}^{-1}\widetilde{\boldsymbol{A}}$ (Hamilton et al., 2017; Li et al., 2018; Schlichtkrull et al., 2017).

2.2 DropEdge

DropEdge is a random data augmentation technique that works by sampling a subgraph of the original input graph in each layer, and uses that for message passing (Rong et al., 2020):

$$\begin{aligned} \mathbf{M}^{(\ell)} &\sim \{\text{Bern}(1-q)\}^{N \times N} \\ \widetilde{\boldsymbol{A}}^{(\ell)} &= \mathbf{M}^{(\ell)} \circ \boldsymbol{A} + \boldsymbol{I}_N \end{aligned} \tag{2.3}$$

Several variants of DropEdge have also been proposed, forming a family of random edge-dropping algorithms for tackling the over-smoothing problem. For example, DropNode (Feng et al., 2020) independently samples nodes and sets their representations to 0, followed by rescaling to make the feature matrix unbiased. This is equivalent to setting the corresponding columns of the propagation matrix to 0. In a similar vein, DropAgg (Jiang et al., 2023) samples nodes that don't aggregate messages from their neighbors. This is equivalent to dropping the corresponding rows of the adjacency matrix. Combining these two approaches, DropGNN (Papp et al., 2021) samples nodes which neither propagate nor aggregate messages in a given message-passing step. These algorithms alleviate over-smoothing by reducing the number of messages being propagated in the graph, thereby slowing down the convergence of node representations.

2.3 Over-squashing

Over-squashing refers to the problem of information from exponentially growing neighborhoods (Chen et al., 2018a) being squashed into finite-sized node representations (Alon & Yahav, 2021). This results in a loss of information as it is propagated over long distances, disallowing MPNNs from capturing long-range interactions (LRIs) and limiting their applications to short-range tasks. Topping et al. (2022) formally characterized over-squashing in terms of the Jacobian of the node-level representations w.r.t. the input features: $\|\partial \boldsymbol{z}_i^{(L)} / \partial \boldsymbol{x}_j\|_1$. Accordingly, over-squashing can be understood as low sensitivity between distant nodes, i.e. small perturbations in a node's features don't effect other distant nodes' representations.

Several works have linked over-squashing in an MPNN with topological properties like Cheeger's constant (Giraldo et al., 2023; Karhadkar et al., 2023), curvature of edges (Liu et al., 2023; Nguyen et al., 2023; Topping et al., 2022), effective resistance between nodes (Arnaiz-Rodríguez et al., 2022;

Black et al., 2023) and the expected commute time between them (Di Giovanni et al., 2023; Giovanni et al., 2024). These results have inspired the design of several graph rewiring techniques that strategically add edges to improve the connectivity in the graph, thereby alleviating over-squashing.

3 Sensitivity Analysis

In this section, we perform a theoretical analysis of the expectation – w.r.t. random edge masks – of sensitivity of node representations. This will allow us to predict how DropEdge-variants affect communication between nodes at various distances, which is relevant for predicting their suitability towards learning LRIs.

3.1 Linear GCNs

We start our analysis with linear GCNs, and treat more general MPNN architectures in the following subsection. In this model, the final node representations can be summarised as

$$\boldsymbol{Z}^{(L)} = \left(\prod_{\ell=1}^{L} \hat{\boldsymbol{A}}^{(\ell)}\right) \boldsymbol{X}\boldsymbol{W} \in \mathbb{R}^{N \times H^{(L)}} \tag{3.1}$$

where $\boldsymbol{W} \coloneqq \prod_{\ell=1}^{L} \boldsymbol{W}^{(\ell)} \in \mathbb{R}^{H^{(0)} \times H^{(L)}}$. Using the i.i.d. assumption on the distribution of edge masks in each layer, the expected sensitivity of node i to node j can be shown to be

$$\mathbb{E}_{\mathbf{M}^{(1)},\ldots,\mathbf{M}^{(L)}}\left[\left\|\frac{\partial \boldsymbol{z}_i^{(L)}}{\partial \boldsymbol{x}_j}\right\|_1\right] = \left(\mathbb{E}\left[\hat{\boldsymbol{A}}\right]^L\right)_{ij} \|\boldsymbol{W}\|_1 \tag{3.2}$$

To keep things simple, we will ignore the effect of DropEdge-variants on the optimization trajectory. Accordingly, it is sufficient to study $\mathbb{E}[\hat{\boldsymbol{A}}]$ in order to predict their effect on over-squashing. To maintain analytical tractability, we assume the use of an asymmetrically normalized adjacency matrix for message-passing, $\hat{\boldsymbol{A}} = \hat{\boldsymbol{A}}^{\text{asym}}$.

Lemma 3.1. *The expected propagation matrix under DropEdge is given as:*

$$\begin{aligned} \dot{\boldsymbol{P}}_{ii} &\coloneqq \mathbb{E}_{\mathsf{DE}}\left[\hat{\boldsymbol{A}}_{ii}\right] = \frac{1-q^{d_i+1}}{(1-q)\,(d_i+1)} \\ \dot{\boldsymbol{P}}_{ij} &\coloneqq \mathbb{E}_{\mathsf{DE}}\left[\hat{\boldsymbol{A}}_{ij}\right] = \frac{1}{d_i}\left(1 - \frac{1-q^{d_i+1}}{(1-q)\,(d_i+1)}\right) \end{aligned} \tag{3.3}$$

where $q \in [0,1)$ is the dropping probability.

See Appendix A.1 for a proof.

Other Variants. We will similarly derive the expected propagation matrix for other random edge-dropping algorithms. First off, DropNode (Feng et al., 2020) samples nodes and drops corresponding columns from the aggregation matrix directly, followed by rescaling of its entries:

$$\mathbb{E}_{\mathsf{DN}}\left[\frac{1}{1-q}\hat{\boldsymbol{A}}\right] = \frac{1}{1-q} \times (1-q)\,\hat{\boldsymbol{A}} = \hat{\boldsymbol{A}} \tag{3.4}$$

That is, the expected propagation matrix is the same as in a NoDrop model ($q = 0$).

Nodes sampled by DropAgg (Jiang et al., 2023) don't aggregate messages. Therefore, if $\hat{\boldsymbol{A}} = \hat{\boldsymbol{A}}^{\text{asym}}$, then the expected propagation matrix is given by

$$\begin{aligned} \mathbb{E}_{\mathsf{DA}}\left[\hat{\boldsymbol{A}}_{ii}\right] &= q + \frac{1-q}{d_i+1} = \frac{1+d_i q}{d_i+1} > \mathbb{E}_{\mathsf{DE}}\left[\hat{\boldsymbol{A}}_{ii}\right] \\ \mathbb{E}_{\mathsf{DA}}\left[\hat{\boldsymbol{A}}_{ij}\right] &= \frac{1}{d_i}\left(1 - \mathbb{E}_{\mathsf{DA}}\left[\hat{\boldsymbol{A}}_{ii}\right]\right) < \mathbb{E}_{\mathsf{DE}}\left[\hat{\boldsymbol{A}}_{ij}\right] \end{aligned} \tag{3.5}$$

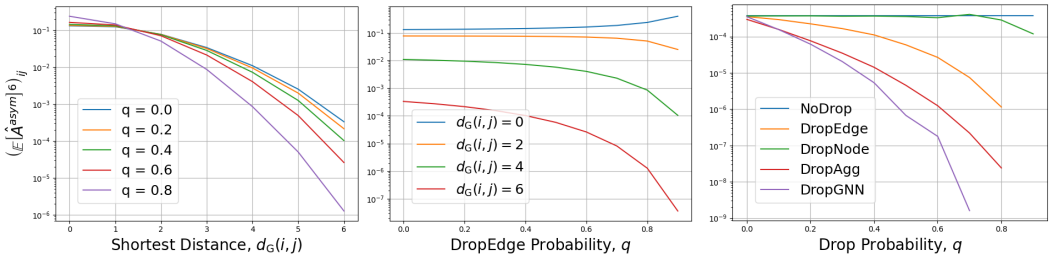

Figure 1: Entries of $\dot{\boldsymbol{P}}^6$, averaged over molecular graphs sampled from the Proteins dataset. *Left*: Sensitivity between nodes decays at a polynomial rate w.r.t. their distance. *Middle*: Similarly, it decays at a polynomial rate w.r.t. the DropEdge probability. *Right*: It decays more quickly with DropAgg than with DropEdge, and even more rapidly with DropGNN.

Finally, DropGNN (Papp et al., 2021) samples nodes which neither propagate nor aggregate messages. From any node's perspective, if it is not sampled, then its aggregation weights are computed as for DropEdge:

$$\begin{aligned} \mathbb{E}_{\mathsf{DG}}\left[\hat{\boldsymbol{A}}_{ii}\right] &= q + (1-q)\,\mathbb{E}_{\mathsf{DE}}\left[\hat{\boldsymbol{A}}_{ii}\right] = q + \frac{1-q^{d_i+1}}{d_i+1} > \mathbb{E}_{\mathsf{DA}}\left[\hat{\boldsymbol{A}}_{ii}\right] \\ \mathbb{E}_{\mathsf{DG}}\left[\hat{\boldsymbol{A}}_{ij}\right] &= \frac{1}{d_i}\left(1 - \mathbb{E}_{\mathsf{DG}}\left[\hat{\boldsymbol{A}}_{ii}\right]\right) < \mathbb{E}_{\mathsf{DA}}\left[\hat{\boldsymbol{A}}_{ij}\right] \end{aligned} \tag{3.6}$$

1-Layer Linear GCNs. $\forall q \in (0,1)$ we have

$$\begin{aligned} \dot{\boldsymbol{P}}_{ii} &= \frac{1}{d_i+1}\sum_{k=0}^{d_i} q^k > \frac{1}{d_i+1} \\ \dot{\boldsymbol{P}}_{ij} &= \frac{1}{d_i}\left(1 - \dot{\boldsymbol{P}}_{ii}\right) < \frac{1}{d_i+1} \end{aligned} \tag{3.7}$$

where the right-hand sides of the two inequalities are the corresponding entries in the propagation matrix of a NoDrop model. Equation 3.3 to Equation 3.7 together imply the following result:

Lemma 3.2. *In a 1-layer linear GCN with $\hat{\boldsymbol{A}} = \hat{\boldsymbol{A}}^{asym}$, using DropEdge, DropAgg or DropGNN*

1. *increases the sensitivity of a node's representations to its own input features, and*
2. *decreases the sensitivity to its neighbors' features.*

In other words, DropEdge-variants prevent a 1-layer GCN from fully utilizing neighborhood information when learning node representations. Ignoring the graph topology this way makes the model resemble an MLP, limiting its expressiveness and hindering its ability to model graph-data.

L-layer Linear GCNs. Unfortunately, we cannot draw similar conclusions in L-layer networks, for nodes at arbitrary distances. To see this, view $\dot{\boldsymbol{P}}$ as the transition matrix of a non-uniform random walk. This walk has higher self-transition ($i = j$) probabilities than in a uniform augmented random walk ($\boldsymbol{P} = \hat{\boldsymbol{A}}^{\text{asym}}$, $q = 0$), but lower inter-node ($i \neq j$) transition probabilities. Note that $\dot{\boldsymbol{P}}^L$ and $\boldsymbol{P}^L$ store the L-step transition probabilities in the corresponding walks. Then, since the paths connecting the nodes $i \in \mathcal{V}$ and $j \in \mathbb{B}^{(L-1)}(i)$ may involve self-loops, $(\dot{\boldsymbol{P}}^L)_{ij}$ may be lower or higher than $(\boldsymbol{P}^L)_{ij}$. Therefore, we cannot conclude how sensitivity between nodes separated by at most $L-1$ hops changes. For nodes L-hops away, however, we can show that DropEdge always decreases the corresponding entry in $\dot{\boldsymbol{P}}^L$, reducing the effective reachability of GCNs. Using Equation 3.5 and Equation 3.6, we can show the same for DropAgg and DropGNN, respectively.

Theorem 3.1. *In an L-layer linear GCN with $\hat{\boldsymbol{A}} = \hat{\boldsymbol{A}}^{asym}$, using DropEdge, DropAgg or DropGNN decreases the sensitivity of a node $i \in \mathcal{V}$ to another node $j \in \mathbb{S}^{(L)}(i)$, thereby reducing its effective receptive field. Moreover, the sensitivity monotonically decreases as the dropping probability is increased.*

See Appendix A.2 for a proof.

Nodes at Arbitrary Distances. Although no general statement could be made about the change in sensitivity between nodes up to $L-1$ hops away, we can analyze such pairs empirically. We sampled 100 molecular graphs from the Proteins dataset (Dobson & Doig, 2003), binned the node-pairs in each graph by the shortest distance between them, and then plotted the average of the corresponding entries in $\dot{\boldsymbol{P}}^L$, $L = 6$.

The results are shown in Figure 1. In the left subfigure, we observe that the sensitivity between two nodes decays at a *polynomial* rate with increasing distance between them. Moreover, DropEdge increases the expected sensitivity between nodes close to each other (0-hop and 1-hop neighbors) in the original topology, but reduces it between nodes farther off. In the middle subfigure, we show how the average sensitivity at different distances changes with the DropEdge probability. Specifically, we observe that the decay in sensitivity to nodes at large distances is polynomial in the DropEdge probability, which suggests that the algorithm would not be suitable for capturing LRIs. Similar conclusions can be made with the symmetrically normalized propagation matrix (see Appendix C.1). Finally, in the right subfigure, we compare the DropEdge-variants by plotting the sensitivity at $d_{\mathcal{G}}(i, j) = L = 6$. Although the analytical form of all the expected propagation matrices are available to us, we approximate them using Monte-Carlo sampling. As expected from Equation 3.5, we observe that DropAgg not only decreases the sensitivity of node representations to distant nodes, but does it to a greater extent than DropEdge. Similarly, Equation 3.6 suggested that DropGNN could be even more harmful than DropAgg, and this is validated by the empirical results. In fact, for $q > 0.7$, nodes 6-hops away are mostly insensitive to each other.

3.2 Nonlinear MPNNs

While linear networks are useful in simplifying the theoretical analysis, they are often not practical. In this subsection, we will consider the upper bounds on sensitivity established in previous works, and extend them to the DropEdge setting.

ReLU GCNs. Xu et al. (2018) considered the case of ReLU nonlinearity, so that the update rule is $\boldsymbol{Z}^{(\ell)} = \mathsf{ReLU}(\hat{\boldsymbol{A}}\boldsymbol{Z}^{(\ell-1)}\boldsymbol{W}^{(\ell)})$. Additionally, it makes the simplifying assumption that each path in the computational graph is *active* with a fixed probability, ρ (Kawaguchi, 2016, Assumption A1p-m). Accordingly, the sensitivity (in expectation) between any two nodes is given as

$$\left\| \mathbb{E}_{\mathsf{ReLU}} \left[\frac{\partial \boldsymbol{z}_i^{(L)}}{\partial \boldsymbol{x}_j} \right] \right\|_1 = \left[\rho \left\| \prod_{\ell=1}^{L} \boldsymbol{W}^{(\ell)} \right\|_1 \right] \left(\hat{\boldsymbol{A}}^L \right)_{ij} = \zeta_1^{(L)} \left(\hat{\boldsymbol{A}}^L \right)_{ij} \tag{3.8}$$

where $\zeta_1^{(L)}$ is independent of the choice of nodes $i, j \in \mathcal{V}$. Taking an expectation w.r.t. the random edge masks, we get

$$\mathbb{E}_{\mathbf{M}^{(1)},\ldots,\mathbf{M}^{(L)}} \left[\left\| \mathbb{E}_{\mathsf{ReLU}} \left[\frac{\partial \boldsymbol{z}_i^{(L)}}{\partial \boldsymbol{x}_j} \right] \right\|_1 \right] = \zeta_1^{(L)} \mathbb{E}_{\mathbf{M}^{(1)},\ldots,\mathbf{M}^{(L)}} \left[\left(\prod_{\ell=1}^{L} \hat{\boldsymbol{A}}^{(\ell)} \right)_{ij} \right] \tag{3.9}$$

$$= \zeta_1^{(L)} \left(\mathbb{E} \left[\hat{\boldsymbol{A}} \right]^L \right)_{ij} \tag{3.10}$$

Using Theorem 3.1, we conclude that in a ReLU-GCN, DropEdge, DropAgg and DropGNN will reduce the expected sensitivity between nodes L-hops away. Empirical observations in Figure 1 and Figure 4 suggest that we may expect an increase in sensitivity to neighboring nodes, but a significant decrease in sensitivity to those farther away.

Source-only Message Functions. Black et al. (2023, Lemma 3.2) considers MPNNs with aggregation functions of the form

$$\mathsf{Agg}^{(\ell)} \left(\boldsymbol{z}_i^{(\ell-1)}, \left\{ \boldsymbol{z}_j^{(\ell-1)} : j \in \mathbb{S}^{(1)}(i) \right\} \right) = \sum_{j \in \mathbb{B}^{(1)}(i)} \hat{\boldsymbol{A}}_{ij} \mathsf{Msg}^{(\ell)} \left(\boldsymbol{z}_j^{(\ell-1)} \right) \tag{3.11}$$

and Upd and Msg functions with bounded gradients. In this case, the sensitivity between two nodes $i, j \in \mathcal{V}$ can be bounded as

$$\left\| \frac{\partial \boldsymbol{z}_i^{(L)}}{\partial \boldsymbol{x}_j} \right\|_1 \leq \zeta_2^{(L)} \left(\sum_{\ell=0}^{L} \hat{\boldsymbol{A}}^\ell \right)_{ij} \tag{3.12}$$

As before, we can use the independence of edge masks to get an upper bound on the expected sensitivity:

$$\mathbb{E}_{\mathbf{M}^{(1)},\ldots,\mathbf{M}^{(L)}} \left[\left\| \frac{\partial \boldsymbol{z}_i^{(L)}}{\partial \boldsymbol{x}_j} \right\|_1 \right] \leq \zeta_2^{(L)} \left(\mathbb{E}_{\mathbf{M}^{(1)},\ldots,\mathbf{M}^{(L)}} \left[I_N + \sum_{\ell=1}^{L} \prod_{k=1}^{\ell} \hat{\boldsymbol{A}}^{(k)} \right] \right)_{ij} \tag{3.13}$$

$$= \zeta_2^{(L)} \left(\sum_{\ell=0}^{L} \mathbb{E} \left[\hat{\boldsymbol{A}} \right]^\ell \right)_{ij} \tag{3.14}$$

Figure 5 shows the plot of the entries of $\sum_{\ell=0}^{6} \dot{\boldsymbol{P}}^\ell$ (i.e. for DropEdge), as in the upper bound above, with $\hat{\boldsymbol{A}} = \hat{\boldsymbol{A}}^{\text{asym}}$. We observe that the sensitivity between nearby nodes marginally increases, while that between distant nodes notably decreases (similar to Figure 1), suggesting significant over-squashing. Similar observations can be made with $\hat{\boldsymbol{A}} = \hat{\boldsymbol{A}}^{\text{sym}}$, and for other DropEdge-variants.

Source-and-Target Message Functions. Topping et al. (2022, Lemma 1) showed that if the aggregation function is instead given by

$$\mathsf{Agg}^{(\ell)} \left(\boldsymbol{z}_i^{(\ell-1)}, \left\{ \boldsymbol{z}_j^{(\ell-1)} : j \in \mathbb{S}^{(1)}(i) \right\} \right) = \sum_{j \in \mathbb{B}^{(1)}(i)} \hat{\boldsymbol{A}}_{ij} \mathsf{Msg}^{(\ell)} \left(\boldsymbol{z}_i^{(\ell-1)}, \boldsymbol{z}_j^{(\ell-1)} \right) \tag{3.15}$$

then the sensitivity between nodes $i \in \mathcal{V}$ and $j \in \mathbb{S}^{(L)}(i)$ can be bounded as

$$\left\| \frac{\partial \boldsymbol{z}_i^{(L)}}{\partial \boldsymbol{x}_j} \right\|_1 \leq \zeta_3^{(L)} \left(\hat{\boldsymbol{A}}^L \right)_{ij} \tag{3.16}$$

With random edge-dropping, this bound can be adapted as follows:

$$\mathbb{E}_{\mathbf{M}^{(1)},\ldots,\mathbf{M}^{(L)}} \left[\left\| \frac{\partial \boldsymbol{z}_i^{(L)}}{\partial \boldsymbol{x}_j} \right\|_1 \right] \leq \zeta_3^{(L)} \left(\mathbb{E} \left[\hat{\boldsymbol{A}} \right]^L \right)_{ij} \tag{3.17}$$

which is similar to Equation 3.10, only with a different proportionality constant, that is anyway independent of the choice of nodes. Here, again, we invoke Theorem 3.1 to conclude that $(\mathbb{E}[\hat{\boldsymbol{A}}]^L)_{ij}$ decreases monotonically with increasing DropEdge probability q. This implies that, in a non-linear MPNN with $\hat{\boldsymbol{A}} = \hat{\boldsymbol{A}}^{\text{asym}}$, DropEdge lowers the sensitivity bound given above. Empirical results in Figure 4 support the same conclusion for $\hat{\boldsymbol{A}} = \hat{\boldsymbol{A}}^{\text{sym}}$.

Message of the Section: Studying the expected propagation matrix allows us to predict the effect of random edge-dropping methods on information propagation in MPNNs. Specifically, DropEdge, DropAgg and DropGNN increase the sensitivity of nodes to their neighbors, but decrease it to nodes farther off. This suggests that these methods would be unsuitable for long-range tasks, where it is imperative to facilitate communication between distant nodes.

4 Experiments

Our theoretical analysis indicates that DropEdge may degrade the performance of GNNs on tasks that depend on capturing LRIs. In this section, we test this hypothesis by evaluating DropEdge models on both short-range and long-range tasks.

Dataset	Nodes	Edges	Features	Classes	Homophily
Cora	2,708	10,556	1,433	7	0.766
CiteSeer	3,327	9,104	3,703	6	0.627
Chameleon	2,277	36,051	2,325	5	0.062
Squirrel	5,201	216,933	2,089	5	0.025
TwitchDE	9,498	306,276	128	2	0.142

Table 1: Dataset statistics. Number of edges excludes self-loops. Homophily measures from (Lim et al., 2021).

Dropout	GNN	Homophilic		Heterophilic		
		Cora	CiteSeer	Chameleon	Squirrel	TwitchDE
DropEdge	GCN	+0.396	+0.448	−0.723	−0.614	−0.509
	GAT	+0.547	+0.548	−0.236	−0.655	−0.409
DropNode	GCN	−0.320	−0.662	−0.863	−0.790	−0.465
	GAT	−0.706	−0.735	−0.855	−0.300	−0.502
DropAgg	GCN	−0.015	+0.294	−0.334	−0.317	−0.566
	GAT	−0.019	+0.392	−0.353	−0.398	−0.022
DropGNN	GCN	+0.360	+0.468	−0.746	−0.600	−0.671
	GAT	+0.236	+0.525	−0.507	−0.304	−0.139

Table 2: Spearman correlation between dropping probability and test accuracy. Note the positive correlations for homophilic datasets and negative correlations for heterophilic datasets. Results suggest that random edge-dropping, although effective at improving generalization in short-range tasks, is unsuitable for long-range ones.

4.1 SETUP

Datasets. Although identifying whether a task requires modeling LRIs can be challenging, understanding the structure of the datasets can provide some insight. For example, homophilic datasets have local consistency in node labels, i.e. nodes closely connected to each other have similar labels. On the other hand, in heterophilic datasets, nearby nodes often have dissimilar labels. Since DropEdge-variants increase a node's sensitivity to its immediate neighbors and reduces its sensitivity to distant nodes, we expect it to improve performance on homophilic datasets but harm performance on heterophilic ones. In this work, we use Cora (McCallum et al., 2000) and CiteSeer (Giles et al., 1998) as representatives of homophilic datasets (Zhu et al., 2020), and Squirrel, Chameleon and TwitchDE (Rozemberczki et al., 2021) to represent heterophilic datasets (Lim et al., 2021). The networks' statistics are presented in Table 1, where we can note the significantly lower homophily measures of heterophilic datasets.

Models. We use two MPNN architectures, GCN and GAT, to demonstrate the effect of DropEdge. GCN satisfies the model assumptions made in all the theoretical results presented in Section 3, while GAT does not fit into any of them. Therefore, GCN and GAT together provide a broad representation of different MPNN architectures. For GAT, we use 2 attentions heads in order to keep the computational load manageable, while at the same time harnessing the expressiveness of the multi-headed self-attention mechanism. As for the model depth, we vary it as $L = 2, 4, 6, 8$.

Dropping Probability. For all the methods, the dropping probabilities are varied as $q = 0.0, 0.1, \ldots, 0.9$, so as to reliably capture the trends in model accuracy. We adopt the common practice of turning the methods off at test-time ($q = 0$), isolating their effect on optimization and generalization, which our theory does not address.

Other experimental details are reported in Appendix D. We conduct 5 independent runs for each dataset−model−dropout−probability configuration and report the average test accuracy (with early-stopping using the validation set).

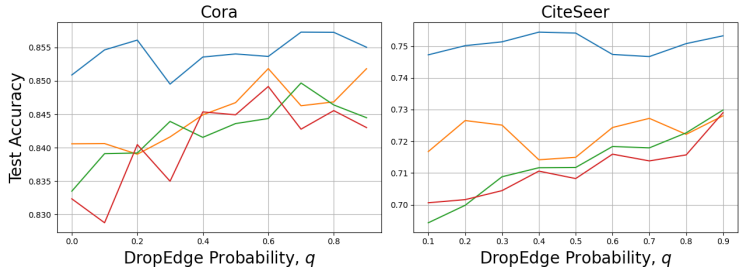

(a) Homophilic datasets

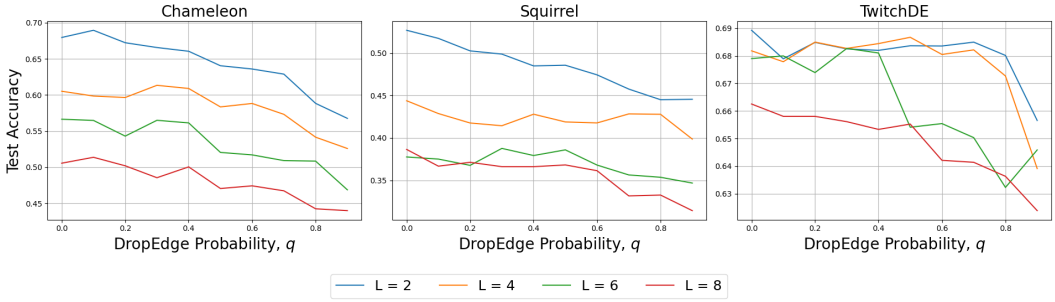

(b) Heterophilic datasets

Figure 2: Dropping probability versus test accuracy of DropEdge-GCN. The theory the explains the contrasting trends as follows: random edge-dropping pushes models to fit to local information during training, which is suitable for short-range tasks, but harms test-time performance in long-range ones.

4.2 RESULTS

In Table 2, we report the rank correlation between the dropping probability and test accuracy of different dataset−model−dropout combinations. The statistics are computed over 10 $(q = 0.0, 0.1, \ldots, 0.9) \times 5$ (samples) $= 50$ runs for each $L = 2, 4, 6, 8$, and then averaged. It is clear to see that in most combinations with the homophilic datasets Cora and CiteSeer, the correlation is positive, indicating that DropEdge and its variants improve test-time performance at short-range tasks. On the other hand, with the heterophilic datasets Chameleon, Squirrel and TwitchDE, the correlation values are negative. This suggests that the edge-dropping methods harm generalization in long-range tasks by forcing the model to overfit to short-range signals.

Figure 2 allows us to visualize these trends for the homophilic and heterophilic datasets. For conciseness, we only display the results for DropEdge-GCNs. Clearly, on Cora and CiteSeer, the model's test-time performance improves with increasing dropping probability, as has been reported earlier. However, on Chameleon, Squirrel and TwitchDE, the performance degrades with increasing dropping probability, as was suggested by our theoretical results. This highlights an important gap in our understanding of dropout methods – while their positive effects on model performance have been well-studied, making them popular choices for training deep GNNs, their evaluation has been limited to short-range tasks, leaving their negative impact on capturing LRIs overlooked.

Remark on DropNode. In Equation 3.4, we noted that DropNode does not suffer from loss in sensitivity. However, note that those results were in expectation. Moreover, our analysis did not account for the effects on the learning trajectory. In practice, a high DropNode probability would make it hard for information in the node features to reach distant nodes. This would prevent the model from learning to effectively combine information from large neighborhoods, harming generalization. In fact, in Table 2, we can see that it is the only dropping method with a negative correlation between dropping probability and test accuracy for each dataset−model combination, including homophilic ones. See Figure 6 for a visualization of its negative effects on test accuracy.

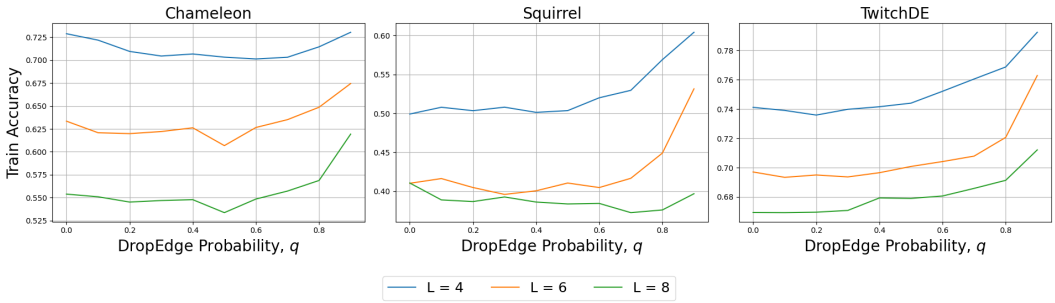

Figure 3: DropEdge probability versus training accuracy of GCNs. The training performance improves with q, suggesting that the models are not underfitting. Instead, the reason for poor test-time performance (Figure 2a) is that models are over-fitting to short-range signals during training, resulting in poor generalization.

4.3 Over-squashing or Under-fitting?

The results in the previous subsection suggest that using random edge-dropping to regularize model training leads to poor test-time performance. We hypothesize that this occurs because the models struggle to propagate information over long distances, causing overfitting of node representations to local neighborhoods. However, a confounding factor is at play: DropEdge variants reduce the generalization gap by preventing overfitting to the training set, which manifests as reduced training performance. If this regularization is too strong, it could lead to underfitting, which could also explain the poor test-time performance on heterophilic datasets. This concern is particularly relevant because the heterophilic networks are much larger than homophilic ones (Table 1), making them more prone to underfitting. To investigate this, we plot the training accuracies of deep DropEdge-GCNs on the heterophilic datasets; Figure 3 shows the results. It is clear that the models do not underfit as the dropping probability increases. In fact, somewhat unexpectedly, the training metrics improve. Together with the results in Figure 2, we conclude that DropEdge-like methods are detrimental in long-range tasks, as they cause overfitting to short-range artifacts in the training data, resulting in poor generalization at test-time.

Message of the Section: Random edge-dropping algorithms reduce the receptive field of MPNNs, forcing them to fit to short-range signals in the training set. While this may make deep GNNs suitable for homophilic datasets, it results in overfitting on heterophilic datasets, which leads to poor test-time performance. Therefore, these methods should be used only after carefully understanding the task at hand.

5 Conclusion

Our analysis points out a key assumption in algorithms designed for training deep GNNs: the idea that if a deep GNN is trainable, it must be able to model LRIs. Our results suggest that this, in fact, need not be true – we theoretically and empirically show that DropEdge-like algorithms exacerbate the over-squashing problem in deep GNNs, and degrade their performance on long-range tasks. Our results highlight a need for a thorough evaluation of methods employed when training deep GNNs, with regards to their capacity to capture LRIs. This will allow us to reliably deploy them in real-life, since we can be assured that the models did not simply overfit to short-range signals.

Limitations. While our theoretical analysis successfully predicts how DropEdge-variants affect test performance on short-range and long-range tasks, it is based on several simplifying assumptions. These assumptions, although standard in the literature, limit the generalizability of our conclusions to other architectures. Specifically, our analysis focuses on certain classes of MPNNs, excluding several GNN architectures specifically designed to enhance long-distance information propagation (see Akansha (2024) for a review).

Practical Considerations. Previous studies have shown that random edge-dropping algorithms can effectively enhance generalization performance in short-range tasks, and our findings support

this conclusion. However, we have also demonstrated that such algorithms can negatively impact over-squashing in MPNNs and harm test-time performance in long-range tasks. Therefore, we recommend exercising caution when using such methods, as careless application can result in models that generalize poorly, which can be detrimental in critical applications.

Future Directions. This work focuses on node-classification tasks, but it is also important to understand the effect of random edge-dropping in other practical settings, e.g. link prediction, and even graph-level tasks. In general, there is a need for a broader investigation into methods designed for training deep GNNs. Specifically, analyzing various strategies designed for mitigating over-smoothing (see Rusch et al. (2023) for a review), particularly in the context of over-squashing, could be invaluable for designing deep GNNs for long-range tasks.

REFERENCES

Singh Akansha. Over-squashing in graph neural networks: A comprehensive survey, 2024.

Uri Alon and Eran Yahav. On the bottleneck of graph neural networks and its practical implications. In *International Conference on Learning Representations*, 2021.

Adrián Arnaiz-Rodríguez, Ahmed Begga, Francisco Escolano, and Nuria M Oliver. Diffwire: Inductive graph rewiring via the lovász bound. In Bastian Rieck and Razvan Pascanu (eds.), *Proceedings of the First Learning on Graphs Conference*, volume 198 of *Proceedings of Machine Learning Research*, pp. 15:1–15:27. PMLR, 12 2022.

Mitchell Black, Zhengchao Wan, Amir Nayyeri, and Yusu Wang. Understanding oversquashing in GNNs through the lens of effective resistance. In Andreas Krause, Emma Brunskill, Kyunghyun Cho, Barbara Engelhardt, Sivan Sabato, and Jonathan Scarlett (eds.), *Proceedings of the 40th International Conference on Machine Learning*, volume 202 of *Proceedings of Machine Learning Research*, pp. 2528–2547. PMLR, 07 2023.

Jianfei Chen, Jun Zhu, and Le Song. Stochastic training of graph convolutional networks with variance reduction. In *International Conference on Machine Learning*, pp. 941–949, 2018a.

Jie Chen, Tengfei Ma, and Cao Xiao. FastGCN: Fast learning with graph convolutional networks via importance sampling. In *International Conference on Learning Representations*, 2018b.

George Dasoulas, Kevin Scaman, and Aladin Virmaux. Lipschitz normalization for self-attention layers with application to graph neural networks. In Marina Meila and Tong Zhang (eds.), *Proceedings of the 38th International Conference on Machine Learning*, volume 139 of *Proceedings of Machine Learning Research*, pp. 2456–2466. PMLR, 18–24 Jul 2021.

Andreea Deac, Marc Lackenby, and Petar Veličković. Expander graph propagation. In *NeurIPS 2022 Workshop: New Frontiers in Graph Learning*, 2022.

Francesco Di Giovanni, Lorenzo Giusti, Federico Barbero, Giulia Luise, Pietro Lio, and Michael M Bronstein. On over-squashing in message passing neural networks: The impact of width, depth, and topology. In *International Conference on Machine Learning*, pp. 7865–7885. PMLR, 2023.

Paul D. Dobson and Andrew J. Doig. Distinguishing enzyme structures from non-enzymes without alignments. *Journal of Molecular Biology*, 330(4):771–783, 2003.

Wenzheng Feng, Jie Zhang, Yuxiao Dong, Yu Han, Huanbo Luan, Qian Xu, Qiang Yang, Evgeny Kharlamov, and Jie Tang. Graph random neural networks for semi-supervised learning on graphs. In H. Larochelle, M. Ranzato, R. Hadsell, M.F. Balcan, and H. Lin (eds.), *Advances in Neural Information Processing Systems*, volume 33, pp. 22092–22103. Curran Associates, Inc., 2020.

Yarin Gal and Zoubin Ghahramani. Bayesian convolutional neural networks with bernoulli approximate variational inference, 2016a.

Yarin Gal and Zoubin Ghahramani. Dropout as a bayesian approximation: Representing model uncertainty in deep learning. In Maria Florina Balcan and Kilian Q. Weinberger (eds.), *Proceedings of The 33rd International Conference on Machine Learning*, volume 48 of *Proceedings of Machine Learning Research*, pp. 1050–1059, New York, New York, USA, 06 2016b. PMLR.

Yarin Gal and Zoubin Ghahramani. A theoretically grounded application of dropout in recurrent neural networks. In D. Lee, M. Sugiyama, U. Luxburg, I. Guyon, and R. Garnett (eds.), *Advances in Neural Information Processing Systems*, volume 29. Curran Associates, Inc., 2016c.

Hongyang Gao, Zhengyang Wang, and Shuiwang Ji. Large-scale learnable graph convolutional networks. In *Proceedings of the 24th ACM SIGKDD International Conference on Knowledge Discovery & Data Mining*, pp. 1416–1424. ACM, 2018.

C. Lee Giles, Kurt D. Bollacker, and Steve Lawrence. Citeseer: an automatic citation indexing system. In *Proceedings of the Third ACM Conference on Digital Libraries*, DL '98, pp. 89–98, New York, NY, USA, 1998. Association for Computing Machinery.

Justin Gilmer, Samuel S. Schoenholz, Patrick F. Riley, Oriol Vinyals, and George E. Dahl. Neural message passing for quantum chemistry. In Doina Precup and Yee Whye Teh (eds.), *Proceedings of the 34th International Conference on Machine Learning*, volume 70 of *Proceedings of Machine Learning Research*, pp. 1263–1272. PMLR, 08 2017.

Francesco Di Giovanni, T. Konstantin Rusch, Michael Bronstein, Andreea Deac, Marc Lackenby, Siddhartha Mishra, and Petar Veličković. How does over-squashing affect the power of GNNs? *Transactions on Machine Learning Research*, 2024.

Jhony H. Giraldo, Konstantinos Skianis, Thierry Bouwmans, and Fragkiskos D. Malliaros. On the trade-off between over-smoothing and over-squashing in deep graph neural networks. In *Proceedings of the 32nd ACM International Conference on Information and Knowledge Management*, CIKM '23, pp. 566–576, New York, NY, USA, 2023. Association for Computing Machinery.

Will Hamilton, Zhitao Ying, and Jure Leskovec. Inductive representation learning on large graphs. In I. Guyon, U. Von Luxburg, S. Bengio, H. Wallach, R. Fergus, S. Vishwanathan, and R. Garnett (eds.), *Advances in Neural Information Processing Systems*, volume 30. Curran Associates, Inc., 2017.

Kaiming He, Xiangyu Zhang, Shaoqing Ren, and Jian Sun. Deep residual learning for image recognition. In *2016 IEEE Conference on Computer Vision and Pattern Recognition (CVPR)*, pp. 770–778, 2016.

Bo Jiang, Yong Chen, Beibei Wang, Haiyun Xu, and Bin Luo. Dropagg: Robust graph neural networks via drop aggregation. *Neural Networks*, 163:65–74, 2023.

Kedar Karhadkar, Pradeep Kr. Banerjee, and Guido Montufar. FoSR: First-order spectral rewiring for addressing oversquashing in GNNs. In *The Eleventh International Conference on Learning Representations*, 2023.

Kenji Kawaguchi. Deep learning without poor local minima. In D. Lee, M. Sugiyama, U. Luxburg, I. Guyon, and R. Garnett (eds.), *Advances in Neural Information Processing Systems*, volume 29. Curran Associates, Inc., 2016.

Diederik Kingma and Jimmy Ba. Adam: A method for stochastic optimization. In *International Conference on Learning Representations (ICLR)*, San Diega, CA, USA, 2015.

Thomas N. Kipf and Max Welling. Semi-supervised classification with graph convolutional networks. In *International Conference on Learning Representations (ICLR)*, 2017.

Yann LeCun, Bernhard Boser, John Denker, Donnie Henderson, R. Howard, Wayne Hubbard, and Lawrence Jackel. Handwritten digit recognition with a back-propagation network. In D. Touretzky (ed.), *Advances in Neural Information Processing Systems*, volume 2. Morgan-Kaufmann, 1989.

Qimai Li, Zhichao Han, and Xiao-ming Wu. Deeper insights into graph convolutional networks for semi-supervised learning. *Proceedings of the AAAI Conference on Artificial Intelligence*, 32(1), 04 2018.

Yujia Li, Daniel Tarlow, Marc Brockschmidt, and Richard S. Zemel. Gated graph sequence neural networks. In Yoshua Bengio and Yann LeCun (eds.), *4th International Conference on Learning Representations, ICLR 2016, San Juan, Puerto Rico, May 2-4, 2016, Conference Track Proceedings*, 2016.

Derek Lim, Xiuyu Li, Felix Hohne, and Ser-Nam Lim. New benchmarks for learning on non-homophilous graphs. *arXiv preprint arXiv:2104.01404*, 2021.

Yang Liu, Chuan Zhou, Shirui Pan, Jia Wu, Zhao Li, Hongyang Chen, and Peng Zhang. Curvdrop: A ricci curvature based approach to prevent graph neural networks from over-smoothing and over-squashing. In *Proceedings of the ACM Web Conference 2023*, WWW '23, pp. 221–230, New York, NY, USA, 2023. Association for Computing Machinery.

Andrew Kachites McCallum, Kamal Nigam, Jason Rennie, and Kristie Seymore. Automating the construction of internet portals with machine learning. *Information Retrieval*, 3(2):127–163, 07 2000.

Federico Monti, Michael Bronstein, and Xavier Bresson. Geometric matrix completion with recurrent multi-graph neural networks. In I. Guyon, U. Von Luxburg, S. Bengio, H. Wallach, R. Fergus, S. Vishwanathan, and R. Garnett (eds.), *Advances in Neural Information Processing Systems*, volume 30. Curran Associates, Inc., 2017.

Khang Nguyen, Hieu Nong, Vinh Nguyen, Nhat Ho, Stanley Osher, and Tan Nguyen. Revisiting over-smoothing and over-squashing using ollivier-ricci curvature. In *Proceedings of the 40th International Conference on Machine Learning*, ICML'23. JMLR.org, 2023.

Kenta Oono and Taiji Suzuki. Graph neural networks exponentially lose expressive power for node classification. In *International Conference on Learning Representations*, 2020.

Pál András Papp, Karolis Martinkus, Lukas Faber, and Roger Wattenhofer. Dropgnn: Random dropouts increase the expressiveness of graph neural networks. In M. Ranzato, A. Beygelzimer, Y. Dauphin, P.S. Liang, and J. Wortman Vaughan (eds.), *Advances in Neural Information Processing Systems*, volume 34, pp. 21997–22009. Curran Associates, Inc., 2021.

Yu Rong, Wenbing Huang, Tingyang Xu, and Junzhou Huang. Dropedge: Towards deep graph convolutional networks on node classification. In *International Conference on Learning Representations*, 2020.

Benedek Rozemberczki, Carl Allen, and Rik Sarkar. Multi-Scale Attributed Node Embedding. *Journal of Complex Networks*, 9(2), 2021.

T. Konstantin Rusch, Michael M. Bronstein, and Siddhartha Mishra. A survey on oversmoothing in graph neural networks, 2023.

Franco Scarselli, Marco Gori, Ah Chung Tsoi, Markus Hagenbuchner, and Gabriele Monfardini. The graph neural network model. *IEEE Transactions on Neural Networks*, 20(1):61–80, 2009.

Michael Schlichtkrull, Thomas N. Kipf, Peter Bloem, Rianne van den Berg, Ivan Titov, and Max Welling. Modeling relational data with graph convolutional networks, 2017.

Christian Szegedy, Wei Liu, Yangqing Jia, Pierre Sermanet, Scott Reed, Dragomir Anguelov, Dumitru Erhan, Vincent Vanhoucke, and Andrew Rabinovich. Going deeper with convolutions. In *2015 IEEE Conference on Computer Vision and Pattern Recognition (CVPR)*, pp. 1–9, 2015.

Jake Topping, Francesco Di Giovanni, Benjamin Paul Chamberlain, Xiaowen Dong, and Michael M. Bronstein. Understanding over-squashing and bottlenecks on graphs via curvature. In *International Conference on Learning Representations*, 2022.

Petar Veličković, Guillem Cucurull, Arantxa Casanova, Adriana Romero, Pietro Liò, and Yoshua Bengio. Graph attention networks. In *International Conference on Learning Representations*, 2018.

Nikil Wale and George Karypis. Comparison of descriptor spaces for chemical compound retrieval and classification. In *Sixth International Conference on Data Mining (ICDM'06)*, pp. 678–689, 2006.

Keyulu Xu, Chengtao Li, Yonglong Tian, Tomohiro Sonobe, Ken-ichi Kawarabayashi, and Stefanie Jegelka. Representation learning on graphs with jumping knowledge networks. In Jennifer Dy and Andreas Krause (eds.), *Proceedings of the 35th International Conference on Machine Learning*, volume 80 of *Proceedings of Machine Learning Research*, pp. 5453–5462. PMLR, 07 2018.

Han Xuanyuan, Tianxiang Zhao, and Dongsheng Luo. Shedding light on random dropping and oversmoothing. In *NeurIPS 2023 Workshop: New Frontiers in Graph Learning*, 2023.

Rex Ying, Ruining He, Kaifeng Chen, Pong Eksombatchai, William L. Hamilton, and Jure Leskovec. Graph convolutional neural networks for web-scale recommender systems. In *Proceedings of the 24th ACM SIGKDD International Conference on Knowledge Discovery & Data Mining*, KDD '18, pp. 974–983, New York, NY, USA, 2018. Association for Computing Machinery.

Yuning You, Tianlong Chen, Yongduo Sui, Ting Chen, Zhangyang Wang, and Yang Shen. Graph contrastive learning with augmentations. In H. Larochelle, M. Ranzato, R. Hadsell, M.F. Balcan, and H. Lin (eds.), *Advances in Neural Information Processing Systems*, volume 33, pp. 5812–5823. Curran Associates, Inc., 2020a.

Yuning You, Tianlong Chen, Zhangyang Wang, and Yang Shen. When does self-supervision help graph convolutional networks? In Hal Daumé III and Aarti Singh (eds.), *Proceedings of the 37th International Conference on Machine Learning*, volume 119 of *Proceedings of Machine Learning Research*, pp. 10871–10880. PMLR, 07 2020b.

Yuning You, Tianlong Chen, Zhangyang Wang, and Yang Shen. L2-gcn: Layer-wise and learned efficient training of graph convolutional networks. In *2020 IEEE/CVF Conference on Computer Vision and Pattern Recognition (CVPR)*, pp. 2124–2132, 2020c.

Yuning You, Tianlong Chen, Zhangyang Wang, and Yang Shen. Bringing your own view: Graph contrastive learning without prefabricated data augmentations. In *Proceedings of the Fifteenth ACM International Conference on Web Search and Data Mining*, WSDM '22, pp. 1300–1309, New York, NY, USA, 2022. Association for Computing Machinery.

Wenqing Zheng, Edward W Huang, Nikhil Rao, Sumeet Katariya, Zhangyang Wang, and Karthik Subbian. Cold brew: Distilling graph node representations with incomplete or missing neighborhoods. In *International Conference on Learning Representations*, 2022.

Kaixiong Zhou, Xiao Huang, Yuening Li, Daochen Zha, Rui Chen, and Xia Hu. Towards deeper graph neural networks with differentiable group normalization. In *Advances in neural information processing systems*, 2020.

Kuangqi Zhou, Yanfei Dong, Kaixin Wang, Wee Sun Lee, Bryan Hooi, Huan Xu, and Jiashi Feng. Understanding and resolving performance degradation in deep graph convolutional networks. In *Proceedings of the 30th ACM International Conference on Information & Knowledge Management*, pp. 2728–2737, 2021.

Jiong Zhu, Yujun Yan, Lingxiao Zhao, Mark Heimann, Leman Akoglu, and Danai Koutra. Beyond homophily in graph neural networks: Current limitations and effective designs. In H. Larochelle, M. Ranzato, R. Hadsell, M.F. Balcan, and H. Lin (eds.), *Advances in Neural Information Processing Systems*, volume 33, pp. 7793–7804. Curran Associates, Inc., 2020.

Marinka Zitnik and Jure Leskovec. Predicting multicellular function through multi-layer tissue networks. *Bioinformatics*, 33(14):i190–i198, 07 2017.

A PROOFS

In this section, we prove Lemma 3.2 and Theorem 3.1.

A.1 EXPECTED PROPAGATION MATRIX UNDER DROPEDGE

Lemma. *When using DropEdge, the expected propagation matrix is given as:*

$$\mathbb{E}_{\mathsf{DE}}\left[\hat{\boldsymbol{A}}_{ii}^{(1)}\right] = \frac{1-q^{d_i+1}}{(1-q)(d_i+1)}$$
$$\mathbb{E}_{\mathsf{DE}}\left[\hat{\boldsymbol{A}}_{ij}^{(1)}\right] = \frac{1}{d_i}\left(1-\frac{1-q^{d_i+1}}{(1-q)(d_i+1)}\right)$$

where $(j \to i) \in \mathcal{E}$*;* $\dot{\boldsymbol{P}}_{ij} = 0$ *otherwise.*

Proof. Recall that a self-loop is added to the graph *after* the edges are dropped, and then the (asymmetric) normalization is performed. In other words, the self-loop is never dropped.

$$\mathbb{E}_{\mathsf{DE}}\left[\hat{\boldsymbol{A}}_{ii}^{(1)}\right] = \mathbb{E}_{m_1,\ldots,m_{d_i}}\left[\frac{1}{1+\sum_{k=1}^{d_i} m_k}\right] \tag{A.1}$$
$$= \mathbb{E}\left[\frac{1}{1+M_i}\right] \tag{A.2}$$
$$= \sum_{k=0}^{d_i}\binom{d_i}{k}(1-q)^k (q)^{d_i-k}\left(\frac{1}{1+k}\right) \tag{A.3}$$
$$= \frac{1}{(1-q)(d_i+1)}\sum_{k=0}^{d_i}\binom{d_i+1}{k+1}(1-q)^{k+1}(q)^{d_i-k} \tag{A.4}$$
$$= \frac{1}{(1-q)(d_i+1)}\sum_{k=1}^{d_i+1}\binom{d_i+1}{k}(1-q)^{k}(q)^{d_i+1-k} \tag{A.5}$$
$$= \frac{1-q^{d_i+1}}{(1-q)(d_i+1)} \tag{A.6}$$

where where $m_k \sim \text{Bern}(1-q)$ and $M_i \sim \text{Binom}(d_i-1, 1-q)$. Similarly,

$$\mathbb{E}_{\mathsf{DE}}\left[\hat{\boldsymbol{A}}_{ij}^{(1)}\right] = (1-q)\,\mathbb{E}_{m_1,\ldots,m_{d_i-1}}\left[\frac{1}{2+\sum_{k=1}^{d_i-1} m_k}\right] \tag{A.7}$$
$$= (1-q)\sum_{k=0}^{d_i-1}\binom{d_i-1}{k}(1-q)^k (q)^{d_i-1-k}\left(\frac{1}{2+k}\right) \tag{A.8}$$
$$= \sum_{k=0}^{d_i-1}\frac{(d_i-1)!}{(k+2)!\,(d_i-1-k)!}(1-q)^{k+1}(q)^{d_i-1-k}(k+1) \tag{A.9}$$
$$= \sum_{k=2}^{d_i+1}\frac{(d_i-1)!}{(k)!\,(d_i+1-k)!}(1-q)^{k-1}(q)^{d_i+1-k}(k-1) \tag{A.10}$$
$$= \frac{1}{d_i(d_i+1)(1-q)}\sum_{k=2}^{d_i+1}\binom{d_i+1}{k}(1-q)^k (q)^{d_i+1-k}(k-1) \tag{A.11}$$
$$= \frac{1}{d_i(d_i+1)(1-q)}\left[(d_i+1)(1-q)-1+q^{d_i+1}\right] \tag{A.12}$$
$$= \frac{1}{d_i}\left(1-\mathbb{E}_{\mathsf{DE}}\left[\hat{\boldsymbol{A}}_{ii}^{(1)}\right]\right) \tag{A.13}$$

□

A.2 SENSITIVITY IN L-LAYER LINEAR GCNS

Theorem. *In an L-layer linear GCN with $\hat{\boldsymbol{A}} = \hat{\boldsymbol{A}}^{asym}$, using DropEdge, DropAgg or DropGNN decreases the sensitivity of a node $i \in \mathcal{V}$ to another node $j \in \mathbb{S}^{(L)}(i)$, thereby reducing its effective receptive field. Moreover, the sensitivity monotonically decreases as the dropping probability is increased.*

Proof. Recall that $\dot{\boldsymbol{P}}$ can be viewed as the transition matrix of a non-uniform random walk, such that $\dot{\boldsymbol{P}}_{uv} = \mathbb{P}(u \to v)$. Intuitively, since there is no self-loop on any given L-length path connecting nodes i and j (which are assumed to be L-hops away), the probability of each transition on any path connecting these nodes is reduced. Therefore, so is the total probability of transitioning from i to j in exactly L hops.

More formally, denote the set of paths connecting the two nodes by

$$\mathsf{Paths}(j \to i) = \{(u_0, \ldots, u_L) : u_0 = j; u_L = i; (u_{\ell-1} \to u_\ell) \in \mathcal{E}, \forall \ell \in [L]\}$$

The (i, j)-entry in the propagation matrix is given by

$$\left(\dot{\boldsymbol{P}}^L\right)_{ij} = \sum_{(u_0,\ldots,u_L)\in\mathsf{Paths}(j\to i)} \prod_{\ell=1}^{L} \dot{\boldsymbol{P}}_{u_\ell u_{\ell-1}} \tag{A.14}$$

Since there is no self-loop on any of these paths,

$$\left(\dot{\boldsymbol{P}}^L\right)_{ij} = \sum_{(u_0,\ldots,u_L)\in\mathsf{Paths}(j\to i)} \prod_{\ell=1}^{L} \frac{1}{d_{u_\ell}} \left(1 - \frac{1 - q^{d_{u_\ell}+1}}{(1-q)(d_{u_\ell}+1)}\right) \tag{A.15}$$

$$< \sum_{(u_0,\ldots,u_L)\in\mathsf{Paths}(j\to i)} \prod_{\ell=1}^{L} \left(\frac{1}{d_{u_\ell}+1}\right) \tag{A.16}$$

The right hand side of the inequality is the (i, j)-entry in the L^{th} power of the propagation matrix of a NoDrop model. From Equation 3.5 and Equation 3.6, we know that Equation A.16 is true for DropAgg and DropGNN as well. We conclude the first part of the proof using Equation 3.2 – the sensitivity of node i to node j is proportional to $(\dot{\boldsymbol{P}}^L)_{ij}$.

Next, we recall the geometric series for any q:

$$1 + q + \ldots + q^d = \frac{1 - q^{d+1}}{1 - q} \tag{A.17}$$

Each of the terms on the right are increasing in q, hence, all the $\dot{\boldsymbol{P}}_{u_\ell u_{\ell-1}}$ factors are decreasing in q. Using this result with Equation A.14, we conclude the second part of the theorem.

□

B TEST-TIME MONTE-CARLO AVERAGING

In Section 3, we focused on the expected sensitivity of the stochastic representations in models using DropEdge-like regularization strategies. This corresponds to their training-time behavior, wherein the activations are random. At test-time, the standard practice is to turn these methods off by setting $q = 0$. However, this raises the over-smoothing levels back up (Xuanyuan et al., 2023). Another way of making predictions is to perform multiple stochastic forward passes, as during training, and then averaging the model outputs. This is similar to Monte-Carlo Dropout, which is an efficient way of ensemble averaging in MLPs (Gal & Ghahramani, 2016b), CNNs (Gal & Ghahramani, 2016a) and RNNs (Gal & Ghahramani, 2016c). In addition to alleviating over-smoothing, this approach also outperforms the standard implementation (Xuanyuan et al., 2023). We can study the effect of random edge-dropping in this setting by examining the sensitivity of the *expected representations*:

$$\left\| \frac{\partial}{\partial \boldsymbol{x}_j} \mathbb{E}\left[\boldsymbol{z}_i^{(L)}\right] \right\|_1$$

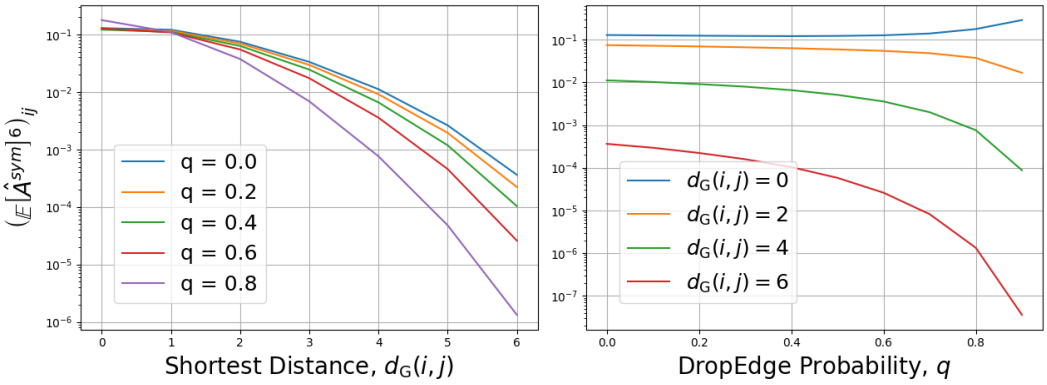

Figure 4: Entries of $\ddot{\boldsymbol{P}}^6$, averaged after binning node-pairs by their shortest distance.

In linear models, the order of the two operations – expectation and sensitivity computation – is irrelevant:

$$\mathbb{E}\left[\left\|\frac{\partial \boldsymbol{z}_i^{(L)}}{\partial \boldsymbol{x}_j}\right\|_1\right] = \left\|\mathbb{E}\left[\hat{\boldsymbol{A}}_{ij}\right]\boldsymbol{W}\right\|_1 = \left\|\mathbb{E}\left[\frac{\partial \boldsymbol{z}_i^{(L)}}{\partial \boldsymbol{x}_j}\right]\right\|_1 = \left\|\frac{\partial}{\partial \boldsymbol{x}_j}\mathbb{E}\left[\boldsymbol{z}_i^{(L)}\right]\right\|_1 \tag{B.1}$$

In general, the two quantities can be related using the convexity of norms and Jensen's inequality:

$$\left\|\frac{\partial}{\partial \boldsymbol{x}_j}\mathbb{E}\left[\boldsymbol{z}_i^{(L)}\right]\right\|_1 \leq \mathbb{E}\left[\left\|\frac{\partial \boldsymbol{z}_i^{(L)}}{\partial \boldsymbol{x}_j}\right\|_1\right] \tag{B.2}$$

Therefore, the discussion in the previous subsections extends to the MC-averaged representations as well. Although tighter bounds may be derived for this setting, we will leave that for future works.

C Additional Figures

In this section, we present some additional figures that demonstrate the negative effects of random edge-dropping, particularly focusing on providing empirical evidence for scenarios not covered by the theory in Section 3.

C.1 Symmetrically Normalized Propagation Matrix

The results in Section 3.1 correspond to the use of $\hat{\boldsymbol{A}} = \hat{\boldsymbol{A}}^{\text{asym}}$ for aggregating messages – in each message passing step, only the in-degree of node i is used to compute the aggregation weights of the incoming messages. In practice, however, it is more common to use the symmetrically normalized propagation matrix, $\hat{\boldsymbol{A}} = \hat{\boldsymbol{A}}^{\text{sym}}$, which ensures that nodes with high degree do not dominate the information flow in the graph (Kipf & Welling, 2017). As in Equation 3.2, we are looking for

$$\mathbb{E}_{\mathbf{M}^{(1)},\ldots,\mathbf{M}^{(L)}}\left[\prod_{l=1}^{L}\hat{\boldsymbol{A}}^{(\ell)}\right] = \ddot{\boldsymbol{P}}^L$$

where $\ddot{\boldsymbol{P}} := \mathbb{E}_{\mathsf{DE}}[\hat{\boldsymbol{A}}^{\text{sym}}]$. While $\ddot{\boldsymbol{P}}$ is analytically intractable, we can approximate it using Monte-Carlo sampling. Accordingly, we use 20 samples of $\mathbf{M}$ to compute an approximation of $\ddot{\boldsymbol{P}}$, and plot out the entries of $\ddot{\boldsymbol{P}}^L$, as we did for $\dot{\boldsymbol{P}}^L$ in Figure 1. The results are presented in Figure 4, which shows that while the sensitivity between nearby nodes is affected to a lesser extent compared to those observed in Figure 1, that between far-off nodes is significantly reduced, same as earlier.

C.2 Upper Bound on Expected Sensitivity

Black et al. (2023) showed that the sensitivity between any two nodes in a graph can be bounded using the sum of the powers of the propagation matrix. In Section 3.2, we extended this bound to random edge-dropping methods with independent edge masks smapled in each layer:

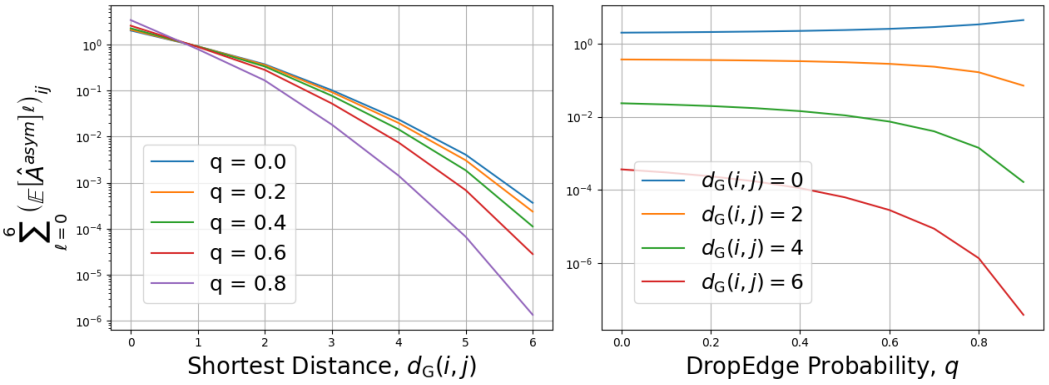

Figure 5: Entries of $\sum_{l=0}^{6} \dot{\boldsymbol{P}}^l$, averaged after binning node-pairs by their shortest distance.

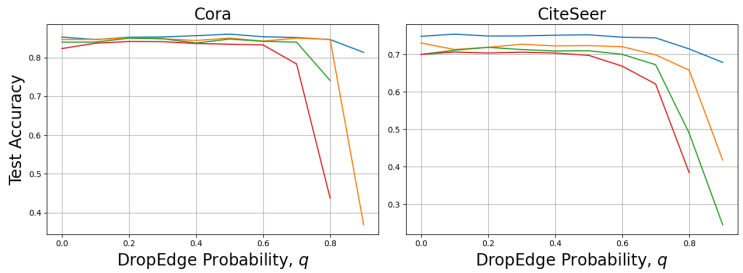

(a) Homophilic datasets

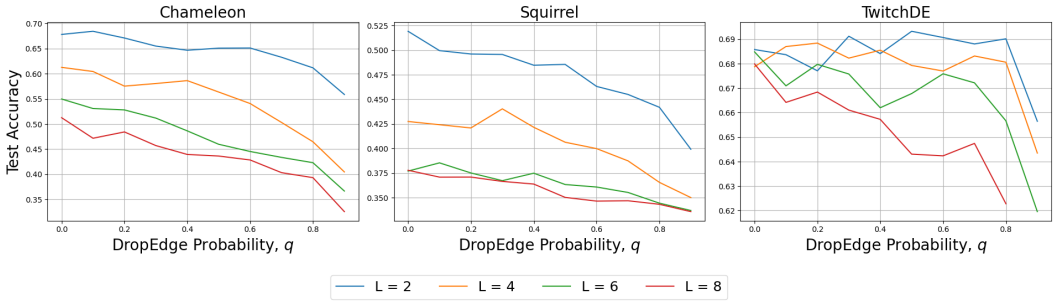

(b) Heterophilic datasets

Figure 6: Dropping probability versus test accuracy of DropNode-GCN.

$$\mathbb{E}_{\mathbf{M}^{(1)},\ldots,\mathbf{M}^{(L)}}\left[\left\|\frac{\partial \boldsymbol{z}_i^{(L)}}{\partial \boldsymbol{x}_j}\right\|_1\right] = \zeta_3^{(L)}\left(\sum_{\ell=0}^{L}\mathbb{E}\left[\hat{\boldsymbol{A}}\right]^{\ell}\right)_{ij}$$

Although this bound does not have a closed form, we can use real-world graphs to study its entries. We randomly sample 100 molecular graphs from the Proteins dataset (Dobson & Doig, 2003) and plot the entries of $\sum_{l=0}^{6} \dot{\boldsymbol{P}}^{\ell}$ (corresponding to DropEdge) against the shortest distance between node-pairs. The results are presented in Figure 5. We observe a polynomial decline in sensitivity as the DropEdge probability increases, suggesting that it is unsuitable for capturing LRIs.

C.3 Test Accuracy versus DropNode Probability

In Equation 3.4, we noted that the expectation of sensitivity remains unchanged when using DropNode. However, these results were only in expectation. In practice, a high DropNode probability

will result in poor communication between distant nodes, preventing the model from learning to effectively model LRIs. This is supported by the results in Table 2, where we observed a negative correlation between the test accuracy and DropNode probability. Moreover, DropNode was the only algorithm which recorded negative correlations on homophilic datasets. In Figure 6, we visualize these relationships, noting the stark contrast with Figure 2, particularly in the trends with homophilic datasets.

D Experiment Details

In this section, we expand on the details of the experiment in Section 4.

Descriptions of the Datasets. Cora (McCallum et al., 2000) and CiteSeer (Giles et al., 1998) are citation networks – their nodes represent scientific publications and an edge between two nodes indicates that one of them has cited the other. The features of each publication are represented by a binary vector, where each index indicates whether a specific word from a dictionary is present or absent. Several studies have showed that these datasets have high homophily in node labels (Lim et al., 2021; Zhu et al., 2020) and that they are modelled much better by shallower networks than by deeper ones (Zhou et al., 2020). Chameleon and Squirrel (Rozemberczki et al., 2021) are networks of English Wikipedia web pages on the respective topics, and the edges between web pages indicate links between them. The task is to predict the average-monthly traffic on each of the web pages. Finally, TwitchDE (Rozemberczki et al., 2021) is a network of Twitch users in Germany, with the edges between them representing their mutual follower relationships. The node features are embeddings of the games played by the users. The task is to predict whether the users use explicit language.

Training Hyperparameters. We standardise most of the hyperparameters across all experiments in order to isolate the effect of dropping probability. Specifically, we fix the size of the hidden representations in each layer at 64, and a linear readout layer is used to compute the node-level logits. The models are trained using the Adam optimizer (Kingma & Ba, 2015), with a learning rate of 3×10^{-3} and a weight decay of 5×10^{-4}, for a total of 300 epochs. For GCN, we use symmetric normalization of the adjacency matrix to compute the edge weights (Kipf & Welling, 2017).

GAT Runs. It is quite problematic to train deep GAT models due to vanishing gradients (Dasoulas et al., 2021). Accordingly, we discard the runs where the model fails to learn, and performs just as well as a random classifier. Specifically, we compute the class distribution in each of the networks, and discard the runs where the test performance does not exceed the maximum proportion. This comes out to be 0.3021, 0.2107, 0.2288, 0.2003 and 0.6045 for Cora, CiteSeer, Chameleon, Squirrel and TwitchDE, respectively.